water

MDPI

Article

Multi-Stage Optimization of Drainage Systems for Integrated Grey–Green Infrastructure under Backward Planning

Chuanhao Sun [1], Qiuyi Rao [2], Mo Wang [1,2,*], Yulu Liu [3], Ziheng Xiong [1], Jiayu Zhao [1], Chengliang Fan [1], Muhammad Adnan Ikram Rana [1], Jianjun Li [1,2] and Menghan Zhang [1,*]

[1] College of Architecture and Urban Planning, Guangzhou University, Guangzhou 510006, China; sunch1110@outlook.com (C.S.); xiongzihengla@outlook.com (Z.X.); zhaoxiaohuazjy@outlook.com (J.Z.); chengliang.fan@gzhu.edu.cn (C.F.); rana@gzhu.edu.cn (M.A.I.R.); lijianjun@gzhu.edu.cn (J.L.)
[2] Architectural Design and Research Institute of Guangzhou University, Guangzhou 510091, China; chewy0917@outlook.com
[3] College of Architecture & Environment, Sichuan University, Chengdu 510641, China
* Correspondence: saupwangmo@gzhu.edu.cn (M.W.); zmh205561@gzhu.edu.cn (M.Z.)

Abstract: In this study, a multi-stage planning framework was constructed by using SWMM simulation modeling and NSGA-II and applied to optimize the layout of integrated grey–green infrastructure (IGGI) under land use change and climate change scenarios. The land use change scenarios were determined based on the master plan of the study area, with imperviousness of 50.7% and 62.0% for stage 1 and stage 2, respectively. Rainfall trends for stage 1 and stage 2 were determined using Earth-E3 from the CMIP6 model. The rainfall in stage 2 increased by 14.9% from stage 1. Based on these two change scenarios, the spatial configuration of IGGI layouts with different degrees of centralization of the layout (DCL) under the two phases was optimized, with the lowest life cycle cost (LCC) as the optimization objective. The results showed that the layout with DCL = 0 had better performance in terms of LCC. The LCC of the layout with DCL = 0 was only 66.9% of that of the layout with DCL = 90.9%. In terms of Tech-R, stage 2 had better performance than stage 1. Furthermore, the average technological resilience (Tech-R) index of stage 2 was 0.8–3.4% higher than that of stage 1. Based on the LCC and Tech-R indices of all of the layouts, TOPSIS was used to compare the performance of the layouts under the two stages, and it was determined that the layout with DCL = 0 had the best economic and performance benefits. The results of this study will be useful in exploring the spatial configuration of urban drainage systems under land use change and climate change for sustainable stormwater management.

Keywords: green infrastructure; backward planning; land use change; climate change; resilience; life cycle cost; multi-stage planning

check for updates

Citation: Sun, C.; Rao, Q.; Wang, M.; Liu, Y.; Xiong, Z.; Zhao, J.; Fan, C.; Rana, M.A.I.; Li, J.; Zhang, M. Multi-Stage Optimization of Drainage Systems for Integrated Grey–Green Infrastructure under Backward Planning. *Water* **2024**, *16*, 1825. https://doi.org/10.3390/w16131825

Academic Editor: Achim A. Beylich

Received: 30 May 2024
Revised: 23 June 2024
Accepted: 25 June 2024
Published: 27 June 2024

Copyright: © 2024 by the authors. Licensee MDPI, Basel, Switzerland. This article is an open access article distributed under the terms and conditions of the Creative Commons Attribution (CC BY) license (https://creativecommons.org/licenses/by/4.0/).

1. Introduction

As a consequence of climate change, exacerbated by the imprudent expansion and intricacies of urbanization, natural calamities have intensified, encompassing phenomena such as rising sea levels, protracted droughts, and the proliferation of urban heat islands [1–3]. In tandem with the aforementioned calamities, this has led to the heightened prevalence of urban pluvial floods worldwide [4]. While urban pluvial flooding may be comparatively less cataclysmic than flash floods or coastal inundation, its heightened frequency and concentration in densely populated areas pose substantive threats to both human welfare and socio-economic stability [5–8]. Specifically, heavy rainfall and urban pluvial floods significantly reduce economic growth; damage infrastructure such as transport, electricity, and communications systems; and even cause human casualties [9]. Urban pluvial floods pose an alarming risk to the sustainable development of cities [10,11]. This challenges planners and decision makers in urban stormwater management [12–14]. It is crucial to establish

urban drainage systems that have strong resilience and adaptability to urban hydrological hazards and maintain sustainable ecosystems and economic development [15,16].

Conventional, cost-intensive grey infrastructure (GREI) and management paradigms have reached a juncture of inadequacy in addressing the burgeoning flood challenges arising from swift urbanization and climate change [17,18]. In such a context, the fusion of GREI combined with rapidly developing green infrastructure (GI) is considered a promising option for sustainable stormwater flood management [14,19,20]. GREI achieves the goal of controlling runoff by rapidly directing surface runoff away from the site and treating it in a centralized manner [21]. On the other hand, GI can achieve ecological sustainability by virtue of its ability to mimic natural hydrological processes [22]. These GI practices can assist GREI through natural retention and infiltration, thereby reducing the runoff coefficients, and the acceptability and reliability of GREI combined with the sustainability and multi-functionality of GI tend to result in better performance than GREI-only or GI-only systems [23–25]. However, in the case of GI, such as bioretention, permeable pavements and green roofs, which have been proposed as small-scale facilities to reduce surface runoff and environmental pollution, their performance in terms of runoff control and peak flow reduction seems to be limited [26,27]. This limitation drastically affects the level of acceptance of GI by governments and private developers and the allocation of investments and space for GI, making the large-scale design and implementation of GI programs almost impossible [28–30]. Furthermore, the strategy of adding multiple outlets to highly centralized GREI systems, dividing the originally concentrated layout into multiple subsystems, has garnered increasing attention in recent years. Under such planning, each subsystem operates independently, significantly alleviating the pressure on drainage systems [31,32]. Moreover, from both water conservation and economic perspectives, decentralized systems prove more attractive than centralized ones [33]. Decentralized systems feature shallower pipeline depths and smaller diameters, which are advantageous for both initial installation and subsequent maintenance. Hence, there is a need to design a decentralized integrated layout in conjunction with GI and GREI for effective and sustainable stormwater management in high-density urban areas.

This integrated layout requires trade-offs between the GREI and GI layout configurations, with numerous options, making it difficult to obtain an optimal layout through manual enumeration and leading to the creation of configurations that are difficult to adapt to regional pressures because manually set configurations rely on subjective experience [34,35]. The advancement of cutting-edge technologies, such as artificial intelligence (AI) algorithms and models, has catalyzed the paradigm shift towards intelligent innovations in urban planning, infrastructure provisioning and hydrological control, offering promising solutions to optimize infrastructure in novel and unprecedented ways [22,36,37]. However, previous studies have predominantly focused on optimizing GI configurations under the assumption of unchanged GREI. For instance, Ghodsi et al. [38] conducted a case study on 897 potential catchment areas in Buffalo, New York, utilizing the Parallel Pareto Archived Dynamically Dimensioned Search (ParaPADDS) algorithm within the novel simulation–optimization tool OSTRICH-SWMM to optimize the positioning of stormwater retention basins. Dong et al. [39] integrated environmental parameters related to greenhouse gas emission mitigation as optimization objective functions, combining them with objective functions related to hydrological and economic benefits, and employed the fast and stable multi-objective optimization algorithm Non-Dominated Sorting Genetic Algorithm II (NSGA-II) as the foundation for the optimization framework. They conducted comprehensive calculations and evaluations of green and gray infrastructure at different locations and scales based on the storm water management model (SWMM), greenhouse gas emission accounting and life cycle cost (LCC) analysis. Liu et al. [34] established a multifunctional evaluation system using water quality remote sensing inversion, SWAT and SWMM simulations, pattern index calculations, LCC, life cycle assessment (LCA) and the NSGA-II optimization algorithm. The optimized solutions obtained possessed several advantages, including regional adaptability, refinement and comparability.

Nevertheless, most of the previous studies have mainly focused on optimal design or hydrological performance assessment for non-stationary events or single rainfall events under the current urban land use stages as well as climatic conditions. For instance, Chen et al. [40] combined SWMM and the Strength Pareto Evolutionary Algorithm 2 to consider the area, location and hydrological performance of GI setups under recurrence periods of 1a, 5a,10a and 20a and seven different rainfall patterns. Tansar et al. [41] used the western district of Pudong, Shanghai, China, as an example of a highly developed urbanized area for the optimization of grey–green infrastructure, where only local climate patterns and urban development plans were included in the study. Unpredictable precipitation events due to global climate change are becoming increasingly common [42,43]. The dynamics of the global water cycle are affected by global warming, and the likelihood and intensity of both extreme and non-extreme rainfall events are potentially aggravated [44,45]. As urban landscapes evolve, there is a notable shift in land use patterns, characterized by a rising proportion of impermeable surfaces [46]. The results of Ye et al. [47] revealed fluctuations in the potential runoff volume and flood area, ranging from −40% to 160% and −40% to 400%, respectively, attributed to variations in rainfall patterns. Additionally, potential changes stemming from alterations in land use ranged from 0% to 3.5% for the runoff volume and 0% to 18% for the flood area. Therefore, grey–green systems designed based on the status quo are often not adaptable and resilient to future scenarios. Saurav et al. [48] showed that the original GI-GREI needs to be upgraded in order to mitigate hydrological stresses as land use forms change. Wang et al. [26] generated integrated GI-GREI (IGGI) layouts for a 10-year return period with a 2 h rainfall scenario and used them to simulate extreme rainfall scenarios with SSP1-2.6, SSP2-4.5 and SSP5-8.5, and these layouts did not show good adaptation. Therefore, there is a need to explore infrastructure forecasting frameworks with adaptability based on based the latest assessment criteria for land use change and climate change trends.

Both climate change and land use change are dynamic processes with stage patterns, and land use change is also characterized by gradual change [49,50]. Therefore, by planning the IGGI system in stages, one can ensure better adaptability to each stage, resulting in a more flexible and dynamic response to the long-term uncertainties of urbanization and climate change [51–53]. In this process, the sequence of planning is crucial to achieve the objectives [54]. In current research, chronological forward planning and reverse chronological backward planning are commonly used in project management [55]. Forward planning is orientated towards objectives, which are continuously optimized and developed, whereas backward planning is orientated towards the final stage and works backwards to the previous stage. Forward planning is better able to anticipate and circumvent problems that may arise in the future, while backward planning is able to generate unique insights and perspectives that traditional forward planning cannot provide [56,57]. The uniqueness of the two planning sequences makes them different in terms of the planning outcomes. However, the current urban drainage systems are generally dominated by forward planning. Therefore, it is necessary to explore an IGGI system generated by backward planning.

Against this background, the current research lacks an IGGI planning framework under future land use change scenarios and climate change scenarios (CCSs), while neglecting the application of backward planning. Therefore, this study aims to fill a critical gap by developing a multi-stage planning framework. This framework is designed to effectively adapt to anticipated changes in land use and climate conditions. Specifically, the objectives of this study are threefold: firstly, to optimize the spatial configuration of IGGI in two stages using a backward planning approach, while incorporating land use change scenarios and CCSs, with constraints focusing on hydraulic reliability; secondly, to evaluate the performance of the optimized IGGI using relevant performance evaluation factors; and, thirdly, to identify the optimal layout across all optimized layouts based on these performance metrics.

2. Methods and Data

In this study, the methodological framework consists of three main components, as illustrated in Figure 1: (1) determining the land use change scenarios under multi-stage planning through the master plan of the study area and determining the CSSs under multi-stage planning using representative SSP scenarios from the EC-Earth model in the CMIP6 model; (2) optimizing the two-stage IGGI layouts based on the backward planning framework to minimize LCC; and (3) evaluating the adaptive quality of the IGGI layouts to cope with extreme rainfall scenarios and determining the optimal IGGI layouts based on LCC and Tech-R.

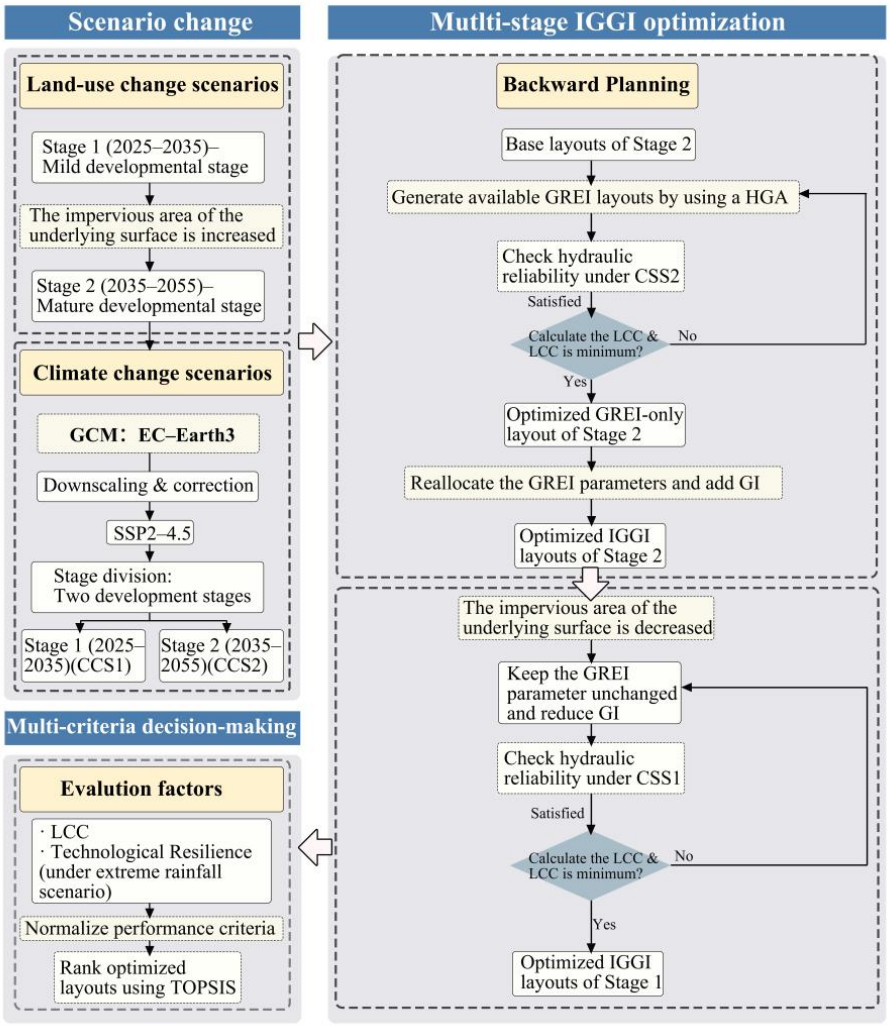

Figure 1. Overview of the framework of this study. Note: GCM refers to Global Climate Model.

2.1. Study Site Description

In this study, the Qianwan Development Area in Shenzhen, China was selected as the case study area (Figure 2). The area has average rainfall of 2000 mm/year and a subtropical monsoon climate, which is expected to last from April to September [58]. Shenzhen, China, as the frontier of China's reform and opening up, has experienced rapid urbanization and achieved a huge increase in its population and economy. Based on the nature of the land use of the Qianwan Area and the distribution of major roads, the basic layout of the Qianwan Area is divided into 52 sub-catchments, 12 potential outlets and 144 pipes, covering an area of more than 300 hectares. A description of each sub-catchment under two stages is provided in Table S1 (Supplementary Materials).

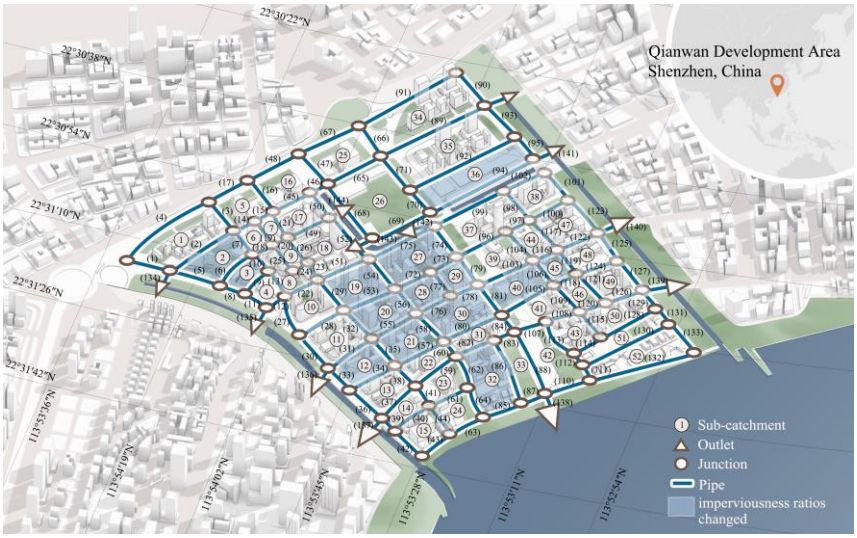

Figure 2. Base layouts of the study site—Qianwan Development Area in Shenzhen, China. Note: the blue color indicates that the sub-catchment has changed its imperviousness ratio during the transition from stage 1 to stage 2.

2.2. Scenario Change Simulations

2.2.1. Land Use Change Scenario

From the beach area in 2010, 40% of the Qianwan area has been completed, and the remaining 60% will be completed in the next 30 years. Assuming construction to a useable state in the next 10 years (2025–2035), the degree of construction is about 75%. This stage is considered to be a lightly developed state, i.e., stage 1. The second stage, from 2035 to 2055, will gradually build up to a fully modern city center with the fully developed development status of a commercial financial center. In terms of urban hydrology, the main difference between the two stages is the change in the surface imperviousness ratio (Table S1). The average imperviousness ratios for stage 1 and stage 2 are 50.7% and 62.0%, respectively.

2.2.2. Climate Change Scenario

In order to obtain the difference in rainfall between stage 1 and stage 2, the present study used the EC-Earth3 model in the CMIP6 model to simulate precipitation, as this is a better predictor of future extreme climatic events. Zamani et al. [59] found that the CMIP6 model showed better performance than CMIP5. Kushwaha et al. [60] assessed 20 CMIP6 models' performance concerning daily precipitation across India, spanning 35 years (1980–2014), during the Indian Summer Monsoon (ISM) season (June to September). They ranked these models using four metrics. Huang et al. [61] compared the applicability of 10 CMIP6 models in simulating the convective afternoon rainfall (CAR) activity in Southeast Asia. The results showed that EC-Earth3 and EC-Earth3-veg are the best two models for the simulation of CAR activity in Southeast Asia. However, due to the relatively coarse spatial resolution of GCMs, statistical downscaling or dynamic downscaling methods are usually required to achieve a certain level of accuracy before they can be used in hydrological–hydraulic impact studies [26]. The EC-Earth3 daily precipitation data applied in this study were downloaded from the NCCS THREDDS Data Catalog (data source: https://ds.nccs.nasa.gov/thredds/catalog/AMES/NEX/GDDP-CMIP6/catalog.html, accessed on 12 May 2024) at a resolution of 0.25° × 0.25°. The two stages are 2025–2035 and 2035–2055, which are the same time periods as the land use change scenario. In order to ensure that the experimental results are representative, the scenario SSP5-8.5 is selected in this study, which refers to a highly energy-intensive development pathway (i.e., SSP5), with the radiative forcing peaking at 8.5 W m^{-2} by 2100 [62].

In this study, the focus is on the daily rainfall data sourced from the EC-Earth3 model. The direct utilization of these datasets for SWMM simulations entails a significant time cost.

Therefore, only stage increments, i.e., the percentage increase in rainfall for stage 2 relative to a single rainfall event for stage 1, are discussed in this study. The daily rainfall data from the EC-Earth3 model were collated to obtain information on the antecedent dry days (ADDs), the number of rainfall events per year and stage, and the average precipitation for a single rainfall event. The degree of change in rainfall was extrapolated by comparing the average rainfall of single rainfall events for the two stages to determine the amount of rainfall for stage 2. Thus, the rainfall event relationship between stage 1 and stage 2 can be expressed as

$$R_{stage\ 2} = R_{stage\ 1} \times \frac{Mean\ Pre_{stage\ 2}}{Mean\ Pre_{stage\ 1}} \quad (1)$$

where $R_{stage\ 2}$ and $R_{stage\ 1}$ denote the design rainfall during the SWMM simulations performed, respectively, where $R_{stage\ 1}$ is set as a 5 y return interval (RI) with a 6 h design rainfall in this study. These data were obtained from the local design criteria for urban drainage systems and the Chicago rain-type formula for Shenzhen, under which the study area would receive 150.7 mm of rainfall in this scenario [63]. *Mean* $Pre_{stage\ 2}$ and Mean *Mean* $Pre_{stage\ 1}$ denote the average rainfall for a single rainfall event, calculated from the daily rainfall data in the EC-Earth3 model, respectively.

2.3. Intelligent Optimization Algorithms for Multi-Stage IGGI

2.3.1. Objective Function Formulations

In order to investigate the optimal GREI and IGGI layouts in backward planning under hydraulic reliability constraints, this study targets the minimum LCC. Throughout the optimization process, several decision variables are involved, including the degree of centralization of the layout (DCL), pipeline arrangement parameters (e.g., pipeline diameter, slope, burial depth) and GI parameters (e.g., type, location and planning). The decision variables were expressed as follows:

$$d_{opt}(d \in D) = \begin{cases} DCL_P(0-100\%) \\ P_k(k = 1-144) \\ A_{i\&j}(i = 1-2; j = 1-52) \end{cases} \quad (2)$$

where is a vector of decision variables for the simulation scenario, d_{opt} is the optimal solution, d is the decision variable, D denotes all feasible options for the system, DCL_p denotes the degree of centralization of the layout, P_k denotes the system pipe arrangement parameters, the value of k denotes all stormwater pipes and $A_{i\&j}$ denotes the area of GI in the sub-catchment, where i denotes the type of GI and j denotes the sub-catchment.

LCC is a comprehensive assessment methodology aimed at quantifying the total expenses encompassing the entire lifespan of a product system. These expenses encompass not only the procurement of materials but also the installation, maintenance and eventual disposal costs [64]. The quantification of LCC involves the utilization of Equations (2)–(4):

$$LCC = Capital_{GREI} + Capital_{PP} + Capital_{BC} + PV_{O\&M-GREI} + PV_{O\&M-GI} \quad (3)$$

$$PVC_{O\&M-GREI} = \sum_{t=0}^{T} O\&M_{GREI} \times \frac{1}{(1+i)^t} \quad (4)$$

$$PVC_{O\&M-GI} = \sum_{t=0}^{T} (O\&M_{PP} + O\&M_{BC}) \times \frac{1}{(1+i)^t} \quad (5)$$

where $Capital_{GREI}$, $Capital_{PP}$ and $Capital_{BC}$ represent the capital cost of GREI, permeable pavement (PP) and bioretention cells (BC), respectively, according to locally available materials and construction/project costs. T denotes the lifespan (years), taken as 30 years. The annual $O\&M_{GREI}$, $O\&M_{PP}$ and $O\&M_{BC}$ costs of GREI, PP and BC account for 10%, 4% and 8% of the capital cost, respectively [65], and i is taken as the discounted present value of 2% in this study [66]. $PVC_{O\&M\text{-}GREI}$ and $PVC_{O\&M\text{-}GI}$ represent the present value of $O\&M$ over the lifespan of GREI and GI, respectively.

2.3.2. Constraints

The structural parameters for each drainage system are specified considering various constraints. Examples include the hydraulic reliability, as well as the practical construction limitations (e.g., pipe burial depth, diameter and slope). In addition, the downstream pipe diameter was constrained to be no smaller than the upstream pipe diameter.

PP and BC, selected for their widespread use and applicability, were used in this study [67]. Typical parameters for both GI practices were designed according to the SWMM design manual [68] (Table S2 in Supplementary Materials). The GI area within the sub-catchment was capped at 10% in consideration of the study area being a densely populated urban commercial center, unsuitable for extensive GI implementation. The above constraints apply to all optimization processes in this study.

2.3.3. Optimal Grey Infrastructure

An initial SWMM is developed utilizing field site data. Subsequently, the graph theoretic algorithm proposed by Bakhshipour et al. [69], known as the Hanging Gardens algorithm, is employed to optimize the layout of the GREI networks across the different DCLs. The DCL is specifically determined by the selection of exits relative to the total number of candidate exits present within the entire system:

$$DCL = 100\% - \frac{N_{SO} - 1}{N_{CO} - 1} \times 100\% \quad (6)$$

where N_{SO} is the number of outlets selected from the list of candidate outlets and N_{CO} is the maximum number of candidate outlets. A lower value of the DCL indicates a greater degree of decentralization in the layout. In this study, DCL = 0 indicates that there are 12 outlets in the layout, DCL = 18.2% indicates that there are 10 outlets in the layout and so on.

The optimization procedure unfolds in a systematic manner: initially, a fully centralized layout, featuring a singular exit from the plethora of potential outlets, is established. Subsequently, leveraging this selected outlet as a pivot, another exit is randomly chosen, prompting the division of the original drainage system. Concurrently, the graph theory algorithm systematically assigns corresponding pipes to each outlet, thereby delineating two freestanding sub-drainage systems. As the system undergoes successive splits, the initially chosen outlet remains fixed, while random selections persist from the remaining outlets, gradually transitioning the original centralized system into a decentralized configuration. After the layout is generated, NSGA-II is used to optimize the pipeline parameters to achieve the minimum LCC according to the constraints in Section 2.3.2. The NSGA-II method facilitated the creation of decision variable scenarios and the computation of objective functions to attain optimal results. Concurrently, the SWMM model aided in computing the objective functions using the decision variable scenarios generated by NSGA-II. The optimization process concludes upon reaching the maximum iteration limit or when the "average spread" stabilizes, indicating the attainment of an optimal solution, i.e., a GREI layout with the lowest LCC and satisfying hydraulic reliability. In this study, the maximum number of iterations is 300 and the total number of samples is 400, which is due to the consideration of the computational efficiency and time cost.

2.3.4. Optimal IGGI Infrastructure

Based on the GREI-only layout generated in the previous section, this study employs the binary encoding scheme of NSGA-II, utilizing binary digits (0 and 1) to represent decision variables. Specifically, the configuration of each GI practice within the sub-catchment is denoted by a binary code. For instance, "00" signifies the absence of GI in the sub-catchment, "01" indicates GI coverage equivalent to 3.3% of the sub-catchment's area, "10" represents 6.7% coverage and "11" denotes 10% coverage. Consequently, these binary codes for all catchments collectively form a "chromosome", analogous to a design solution or scheme. Notably, to control the configurations of BC and PP within each sub-catchment, a total of 4 × NS (number of sub-catchments) binary codes are required. Furthermore, it is

imperative to highlight that if the combined areas of BC and PP within a sub-catchment surpass 10% of the sub-catchment area, they are proportionally reallocated to ensure compliance with the 10% threshold.

The integration of GI within the GREI-only layout plays a pivotal role in runoff management and infiltration enhancement, consequently substituting a segment of the pipeline network. Hence, to fulfill the dual objectives of minimizing the LCC while upholding the hydraulic reliability, it becomes imperative to downsize the diameters of the existing pipes. Analogous to the encoding scheme employed for the GI configuration, the same coding methodology is utilized to govern the pipe adjustments. Each value within the total array of codes, i.e., 2 × NP (number of pipes), is deciphered as follows:

$$P_k \begin{cases} 00 \rightarrow Same\ as\ in\ the\ GREI-only\ scheme \\ 01 \rightarrow One\ size\ smaller\ than\ in\ the\ GREI-only\ scheme \\ 10 \rightarrow Two\ sizes\ smaller\ than\ in\ the\ GREI-only\ scheme \\ 11 \rightarrow Three\ sizes\ smaller\ than\ in\ the\ GREI-only\ scheme \end{cases} \quad (7)$$

where P_k denotes the system pipe parameters and the value of k denotes all stormwater pipes.

2.3.5. Backward Planning

Backward planning involves the iterative reduction of GI in reverse chronological order based on the final development stage (i.e., stage 2) within an urban built-up area. This IGGI system will over-perform in the face of the stage I land use scenario, with an excessive number of GI practices, which will result in unnecessary operation and maintenance costs. Therefore, a reasonable reduction in GI can be achieved to achieve greater economic efficiency while ensuring hydraulic reliability.

Considering the need to ensure that the GREI system does not change during the process of the GI decrease in reverse planning, the same binary coding was used to control the GI increment and decrement in each sub-catchment. Specifically, a combination of two binary codes was deployed to delineate the four matters of GI addition or subtraction, with each combination decoded as follows:

$$Re_{GI} \begin{cases} 00 \rightarrow Unchanged \\ 01 \rightarrow Reduced\ by\ 3.3\% \\ 10 \rightarrow Reduced\ by\ 6.7\% \\ 11 \rightarrow Reduced\ by\ 10.0\% \end{cases} \quad (8)$$

where the reductions of 3.3%, 6.7% and 10.0% are based on the area of the sub-catchment.

2.4. Performance Evaluation Factor

The resilience of infrastructure systems to extreme conditions stands as a pivotal criterion in the assessment of sustainable drainage systems. In this study, the technological resilience (Tech-R) index was employed to gauge the resilience of the infrastructure against severe storm events. A comprehensive set of 9 rainfall scenarios, spanning RIs of 10, 50 and 100 years, coupled with durations of 6 h, 12 h and 18 h, was utilized for evaluation purposes. Table 1 delineates the rainfall depth and maximum intensity for each of the twelve rainfall scenarios. The Tech-R metric operates on a scale ranging from 0 to 100%, where a score of 0 signifies complete susceptibility to the given conditions, while 100% reflects flawless resilience against the rainfall event. The Tech-R value is determined via the following calculation:

$$Tech-R = 100\% - \frac{V_{flooding\ (i)}}{Pre_{(i)} \times A} \times 100\% \quad (9)$$

where A denotes the size of the study area (m^2). $V_{flooding\ (i)}$ and $Pre_{(i)}$ represent the volume of the overflow load (m^3) and precipitation (mm) for a given rainfall event i, respectively.

$Pre_{(i)} \times A$ represents the volume of rainfall (m^3) received by the study site during the rainfall cycle.

Table 1. Rainfall depth and maximum intensity for different rainfall scenarios.

Feature	Rainfall Scenarios								
	10 y RI			50 y RI			100 y RI		
	6 h	12 h	18 h	6 h	12 h	18 h	6 h	12 h	18 h
Rainfall depth (mm)	187.2	256.7	308.3	235.9	323.6	388.6	256.9	352.4	423.2
Maximum intensity (mm/min)	3.6	3.6	3.6	4.6	4.6	4.6	5.0	5.0	5.0

2.5. Decision-Making Based on LCC and Tech-R

TOPSIS, renowned for its efficacy in solving multi-criteria decision-making challenges, offers reliable evaluation results swiftly and with computational efficiency, and it is easy to understand and use [70,71]. This study employs LCC and Tech-R as performance evaluation factors in determining the optimal IGGI scheme for each developmental stage. The weights assigned to LCC and Tech-R maintain a 1:1 ratio, with the Tech-R weights further adjusted based on the duration of the planning stages—10 years for stage 1 and 20 years for stage 2—resulting in respective weights of 16.7% and 33.3% for Tech-R in stages 1 and 2. Additionally, considering nine distinct rainfall scenarios in the Tech-R assessments, the weights for each Tech-R are distributed as 1.9% in stage 1 and 3.7% in stage 2.

3. Results and Discussion

3.1. Climate Simulation and Analysis

A statistical examination of the climatic attributes was performed across the delineated stages, as outlined in Table 2. In stage 1, the average number of rainfall events per year stands at 37.6, with a marginal decrease to 35.8 in stage 2, denoting a modest 4.8% reduction. Notably, while the mean value of ADD exhibits a declining trajectory, the maximum ADD value shows a conspicuous rise, marking a substantial 28.8% increase. Moreover, both the mean and maximum precipitation per rainfall event exhibit an upward trend. Stage 2 notably witnesses a 14.9% augmentation in mean rainfall per event and a notable 27.4% surge in maximum rainfall relative to stage 1. This implies that certain periods may experience more concentrated and intense precipitation events, while others may witness comparatively drier spells, contributing to an overall uneven distribution of rainfall over time. Such an uneven distribution poses significant implications for various sectors, including urban planning and water resource management [5,72].

Table 2. Statistical analysis of climatic characteristics in stages 1 and 2 under SSP5-8.5 scenarios.

Climate Change Scenario		SSP5-8.5	
		Stage 1 (0–10 Years)	Stage 2 (10–30 Years)
Average number of rainfall events per year		37.6	35.8
ADD	Mean (days)	5.3	5.1
	Max (days)	57.0	74.0
Precipitation	Mean (mm)	57.9	66.5
	Max (mm)	382.6	487.6

Note: the Mean and Max values signify the average and maximum rainfall intensities of all rainfall events within each period. A rainfall event is defined as continuous rainfall exceeding 1 mm with intervals of at least 24 h between events.

In alignment with the methodological framework expounded in Section 2.2.2, the hypothetical approach is predicated upon the manipulation of the simulated rainfall parameters. Specifically, optimization stage 1 simulates a 5 y RI and 6 h design rainfall event, yielding a precipitation magnitude of 150.7 mm. Subsequently, the simulated rainfall event

in stage 2 undergoes modification to entail a 6 h design rainfall event with an amplified precipitation amount of 173.2 mm. This adjustment underscores the dynamic nature of precipitation regimes, necessitating tailored modeling strategies to effectively capture the evolving climatic dynamics in urban hydrological contexts.

3.2. IGGI Schemes along Backward Planning

Utilizing the multi-stage IGGI optimization methodology, six distinct layout schemes were derived, spanning from a centralized layout (DCL = 90.9) to a fully decentralized setup (DCL = 0). The detailed investment allocation of the optimized layout, with the goal of backward planning across two developmental stages, is elucidated in Table 3. It is shown that the LCC increases with the increasing centralization of the optimized layout. Specifically, when the DCL = 90.9%, the cumulative expenditure of the two stages reaches 99,269.5 (USD K), while this value is only 66,427.8 (USD K) under the DCL = 0 layout. In the layout of full decentralization, the LCC of the optimized layout amounts to merely 66.9% of its centralized layout. This substantial variance is predominantly due to the adaptability inherent in decentralized arrangements, consequently yielding diminished expenses in infrastructure construction and maintenance [73,74]. Decentralized layouts afford a surplus of proximate outlets, thereby mitigating pipeline lengths, whereas centralized layouts necessitate the proliferation of large-diameter conduits and extensive network spans, thereby incurring escalated construction and maintenance expenses.

Table 3. The LCCs associated with various DCL-optimized layouts within the framework of backward planning.

Planning Stage	Cost (USD K)	Optimized Layout					
		DCL = 90.9%	DCL = 72.7%	DCL = 54.5%	DCL = 36.4%	DCL = 18.2%	DCL = 0
Stage 1 (0–10 years)	CapitalGREI	25,248.7	23,939.0	22,057.9	17,747.4	16,555.4	16,037.1
	$PVC_{O\&M\text{-}GREI}$	22,679.9	21,503.4	19,813.7	15,941.8	14,871.1	14,405.5
	$Capital_{PP}$	5058.1	4913.4	4208.9	5016.8	5253.2	4949.1
	$PVC_{O\&M\text{-}PP}$	1817.4	1765.4	1512.3	1802.6	1887.5	1778.2
	$Capital_{BC}$	410.0	228.2	45.7	30.5	197.6	76.1
	$PVC_{O\&M\text{-}BC}$	294.7	164.0	32.9	21.9	142.0	54.7
	Total cost (stage 1)	55,508.8	52,513.4	47,671.4	40,561.0	38,906.8	37,300.7
Stage 2 (10–30 years)	$PVC_{O\&M\text{-}GREI}$	33,868.4	32,111.5	29,588.1	23,806.2	22,207.2	21,512.0
	$Capital_{PP}$	3094.2	3439.7	3156.4	2899.3	3087.9	2600.1
	$PVC_{O\&M\text{-}PP}$	4374.1	4481.9	3951.9	4247.4	4475.5	4050.6
	$Capital_{BC}$	957.0	744.7	1078.6	699.2	836.0	425.8
	$PVC_{O\&M\text{-}BC}$	1467.0	1044.0	1206.5	783.1	1109.2	538.6
	Total cost (stage 2)	43,760.7	41,821.8	38,981.5	32,435.2	31,715.8	29,127.1
LCC (0–30 years)		99,269.5	94,335.2	86,652.9	72,996.2	70,622.6	66,427.8

Multi-stage planning offers a significant advantage over singular planning endeavors by curbing redundant GI practices in stage I and negating the associated operation and maintenance costs during subsequent periods. Referring to Table 3, the analysis reveals that the expenditure for newly constructed GI in stage II spans from 3025.9 (USD K) to 4235.0 (USD K). These GI practices would have additionally incurred operation and maintenance costs for 0–10 years had they adhered to a one-off decision. In addition, this model of staged planning provides better flexibility, reduces risks, avoids potential losses due to the large one-time investment of resources and is better able to cope with the possible future fine-tuning of the land use [75,76]. Multi-stage planning can be assessed at each stage and adjusted and optimized in light of new circumstances, improving the controllability. Drainage systems are often implemented by the government, and phasing allows for the gradual allocation of funds for implementation, thus reducing the burden of one-time investments and allowing urban planners and decision-makers to use the funds for other projects necessary for the development of the city [77].

Furthermore, regardless of whether it is stage 1 or stage 2, the construction area and costs of PP significantly exceed those of BC (as shown in Table 3). In stage 1, PP and BC accounted for 92.5–99.4% and 0.6–7.5%, respectively, of the total construction

cost of the GI in stage 1, and, in stage 2, this index changed to 74.5–85.9% and 14.1–25.5%. This underscores the substantial economic and hydrological benefits associated with PP in the optimized IGGI layout, rendering it more cost-effective relative to BC. The prevalence of PP in both stages highlights its critical role in achieving efficient resource allocation and optimizing the hydrological performance. The higher construction area and costs of PP underscore its importance and effectiveness in enhancing the overall performance and sustainability of the GI system. Furthermore, this emphasizes the strategic significance of prioritizing PP within the optimized IGGI layout to maximize both the economic and hydrological efficiency, thereby ensuring the long-term effectiveness and viability of the infrastructure.

3.3. Performance Evaluation under Extreme Rainfall Scenarios

The hydrological simulation conducted on the two-stage optimized layout under nine extreme rainfall scenarios using the SWMM produced the Tech-R index, as illustrated in Figure 3. It is evident that, under identical rainfall scenarios, the adaptability of the stage 2 optimized layout surpasses that of stage 1. The average Tech-R index of the stage 2 layout exceeds that of stage 1 by 1.9%, with a maximum difference of 3.4% and a minimum of 0.8%. This superiority in adaptability stems primarily from the meticulous optimization of the stage 2 layouts, integrating an array of additional GI practices beyond what stage 1 entails. These practices not only contribute to improved stormwater management but also demonstrate the potential for sustainable urban development. However, as detailed in the preceding section, implementing stage 2 requires an additional investment ranging from 3025.9 (USD K) to 4235.0 (USD K) over stage 1, despite the marginal increase in Tech-R. Consequently, it becomes imperative to evaluate whether such expenditure is warranted to achieve superior hydrological benefits. This decision should be made on a case-by-case basis, with a comprehensive assessment of the economic and functional advantages, playing a pivotal role in determining the optimal scheme [34,39].

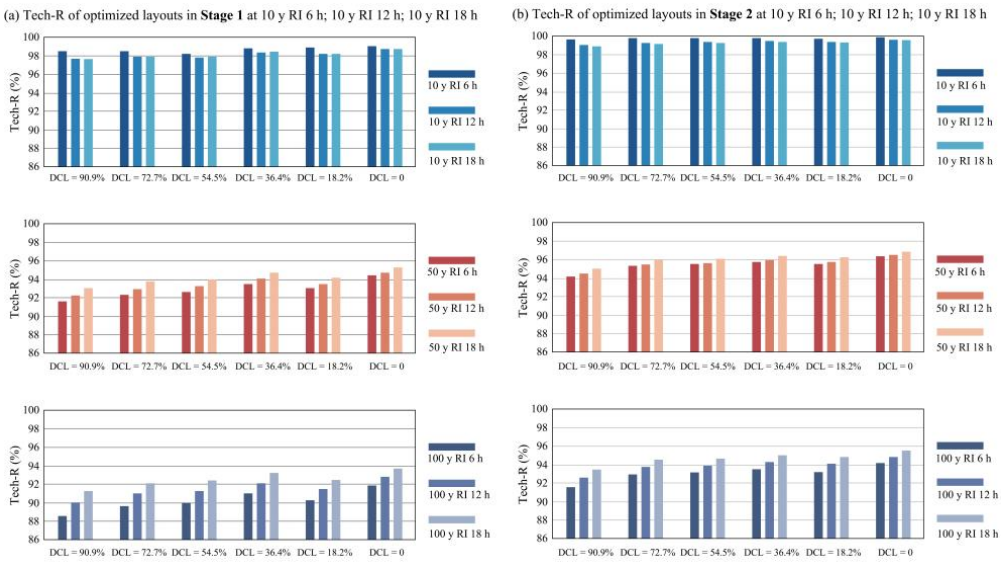

Figure 3. Tech-R of optimized layouts in stage 1 and stage 2 under nine extreme rainfall scenarios.

It is worth noting that the adaptability of the optimized layout to extreme rainfall scenarios gradually increases with a decreasing DCL (increase in the number of outlets) for both stage 1 and stage 2 (Figure 3). This phenomenon underscores the intrinsic advantage of relatively decentralized configurations in exhibiting superior hydrological efficacy, echoing prior findings such as those elucidated by Bakhshipour et al. [69]. For instance, within the context of a 50 y RI and a 12 h rainfall event, the optimized layout with DCL = 0 in stage 1 and 2 had 2.5% and 2.0% higher Tech-R values than the optimized layout with DCL = 90.9%, respectively. However, the correlation between a reduced DCL and an

augmented Tech-R is not unequivocal. Indeed, instances arise where the Tech-R when the layout has DCL = 18.2% does not consistently eclipse that of layouts with a DCL of 36.4%. Illustratively, within the aforementioned 50 y RI and 12 h rainfall scenario, optimized layouts featuring a DCL of 18.2% in both stages exhibit Tech-R values that are marginally lower (by 0.6% and 0.2% in stage 1 and stage 2, respectively) compared to layouts with a DCL of 36.4%. Nevertheless, contextualizing this disparity necessitates the consideration of the variance in the LCC between the two layouts, whereupon the divergence in Tech-R is not considered a significant issue.

Furthermore, concerning RIs of both 50 y and 100 y, there was a discernible inclination for the Tech-R of the optimized layouts to ascend alongside escalating rainfall durations (Figure 3). Exemplarily, under the 100 y RI, the Tech-R values of the optimized layout with DCL = 0 for the 6 h and 18 h rainfall scenarios were 91.9% and 93.7% for stage 1 and 94.2% and 95.6% for stage 2, which increased by 1.8% and 1.4%, respectively. This tendency underscores the evolving adaptability of the optimized layout to the hydrological dynamics in the face of prolonged rainfall events. Such augmentation could be attributed to the fact that a longer rainfall duration provides more time for the hydrological system to process and disperse runoff, allowing the layout to be more efficient [78]. Consequently, this observed trend assumes critical relevance in the realm of urban water resource management and flood defense planning, particularly against the backdrop of the amplified frequency and intensity of extreme climatic phenomena engendered by climate change [79]. It emphasizes the imperative of enhancing the infrastructural robustness and adaptability to respond to changing hydrological dynamics.

3.4. Determination of Optimal IGGI Scheme

The determination of the optimal layout is facilitated by the normalization of the economic performance indices using TOPSIS. The tabulated ranking in Table 4 delineates the optimal layouts under varying DCLs, with the decentralized layout with a DCL of 0 garnering the highest score, while the centralized layout with a DCL of 90.9% attains the lowest score. Evidently, the decentralized layout, characterized by a DCL of 0, emerges as the unequivocal frontrunner, primarily attributable to its superior performance across the economic and hydrological dimensions. However, intriguing nuances surface when examining the intermediate DCL scenarios. Specifically, the layout with a DCL of 18.2%, indicative of a relatively heightened degree of decentralization, fails to outperform its counterpart with a DCL of 36.4%. This discrepancy stems from the pronounced weakness exhibited by the former in the domain of the Tech-R. These findings underscore the multi-dimensional considerations requisite in optimizing the layout configurations, emphasizing the intricate balance between the decentralization schemes and Tech-R to ensure robust and sustainable infrastructural designs.

The visualization of the spatial arrangement of the IGGI for both the lowest-performing (DCL = 90.9%) and highest-performing layouts (DCL = 0) during stage 1 and stage 2 is presented (refer to Figure 4). It can be clearly seen that the layout with a DCL of 0 is significantly smaller than the layout with a DCL of 90.9% in both the average scale and size of the GREI. The layout with a DCL of 0 has average pipe diameters and junction depths measuring 0.61 m and 1.93 m, respectively, while the layout with a DCL of 90.9% has average pipe diameters and node depths of 0.72 m and 2.13 m. This discrepancy underscores the more streamlined and space-efficient nature of the layout with a DCL of 0, indicative of the superior utilization of the infrastructure resources. This optimization of the spatial arrangement manifests in several benefits, notably in reduced construction and maintenance costs over the LCC of the infrastructure. The inherent compactness and efficiency of the layout with a DCL of 0 contribute to enhanced economic viability and sustainability.

Table 4. Ranking results of optimized layouts.

Normalized Evaluation Factor		Optimized Layout						
		DCL						Weight (%)
		90.9%	72.7%	54.5%	36.4%	18.2%	0	
LCC		0	0.15	0.38	0.80	0.87	1	50.0
Stage 1 (0–10 years)	Tech-R (10 y RI 6 h)	0.34	0.35	0	0.73	0.86	1	1.9
	Tech-R (10 y RI 12 h)	0	0.17	0.12	0.65	0.52	1	1.9
	Tech-R (10 y RI 18 h)	0	0.19	0.23	0.68	0.51	1	1.9
	Tech-R (50 y RI 6 h)	0	0.25	0.35	0.67	0.51	1	1.9
	Tech-R (50 y RI 12 h)	0	0.29	0.41	0.73	0.50	1	1.9
	Tech-R (50 y RI 18 h)	0	0.31	0.42	0.74	0.51	1	1.9
	Tech-R (100 y RI 6 h)	0	0.31	0.41	0.73	0.50	1	1.9
	Tech-R (100 y RI 12 h)	0	0.34	0.43	0.75	0.51	1	1.9
	Tech-R (100 y RI 18 h)	0	0.33	0.45	0.77	0.50	1	1.9
Stage 2 (10–30 years)	Tech-R (10 y RI 6 h)	0	0.58	0.58	0.66	0.37	1	3.7
	Tech-R (10 y RI 12 h)	0	0.38	0.52	0.71	0.55	1	3.7
	Tech-R (10 y RI 18 h)	0	0.40	0.54	0.69	0.60	1	3.7
	Tech-R (50 y RI 6 h)	0	0.51	0.61	0.70	0.60	1	3.7
	Tech-R (50 y RI 12 h)	0	0.50	0.58	0.72	0.63	1	3.7
	Tech-R (50 y RI 18 h)	0	0.50	0.57	0.74	0.65	1	3.7
	Tech-R (100 y RI 6 h)	0	0.53	0.61	0.74	0.64	1	3.7
	Tech-R (100 y RI 12 h)	0	0.51	0.57	0.74	0.66	1	3.7
	Tech-R (100 y RI 18 h)	0	0.53	0.57	0.75	0.65	1	3.7
Closeness coefficient		0	0.29	0.43	0.75	0.72	1	-
Ranking order		6	5	4	2	3	1	-

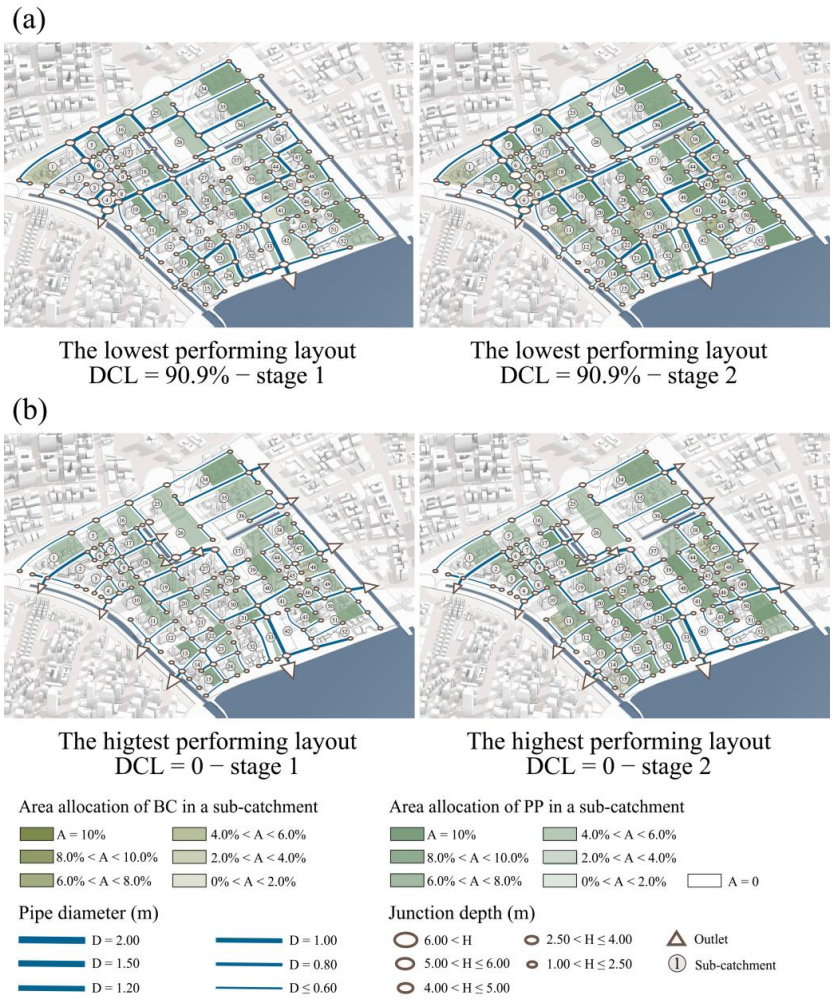

Figure 4. (**a**) Spatial arrangement of the IGGI for both the lowest-performing (DCL = 90.9%), and (**b**) highest-performing layouts (DCL = 0) during stage 1 and stage 2.

4. Conclusions

This study introduces an advanced multi-stage planning framework for urban drainage systems, integrating hydrological modeling and optimization algorithms under a backward planning approach. By addressing the dynamic challenges posed by land use and climate change, the framework aims to optimize the resilience and cost-effectiveness of urban drainage infrastructure.

The key findings demonstrate that staged planning not only reduces the initial costs, particularly in GI operations and maintenance, but also offers unparalleled flexibility for iterative adjustments and optimizations based on the evolving conditions at each planning stage. Furthermore, PP is more suitable for densely urbanized areas, offering significant potential to increase the pervious open land surfaces.

Under extreme rainfall scenarios, the optimized layouts were rigorously evaluated, revealing stage 2′s superior hydrological resilience compared to stage 1, particularly in enhancing the Tech-R metric. The research highlights the advantages of a decentralized layout with a smaller DCL, providing enhanced flood protection and faster adaptation capabilities in extreme weather conditions.

Moreover, the study's innovative approach ranks the optimized layouts based on a comprehensive assessment of the LCC and performance metrics, with layouts featuring a DCL of 0 emerging as significantly advantageous in terms of both economic benefits and operational performance.

By conducting detailed spatial analyses and comparisons between the top-performing and baseline layouts, including considerations of the size, location, dimensions and GI configurations, the study substantiates the efficacy of its multi-stage planning framework. Ultimately, this research contributes a pivotal strategy for the integration of cost-effectiveness with optimal performance in urban drainage systems. It offers a promising pathway to guide sustainable urban development initiatives aimed at enhancing the resilience of water infrastructure amidst evolving environmental and developmental pressures.

Supplementary Materials: The following supporting information can be downloaded at: https://www.mdpi.com/article/10.3390/w16131825/s1, Table S1: Characteristics of sub-catchments in SWMM in case study; Table S2: Values of experimental design of permeable pavement (PP) and bioretention cells (BC) in SWMM.

Author Contributions: Conceptualization, C.S. and M.W.; methodology, C.S., Q.R. and M.W.; software, C.S., Q.R., Y.L. and Z.X.; validation, J.Z., M.A.I.R. and J.L.; formal analysis, M.Z., J.Z. and C.F.; investigation, Q.R., Y.L. and Z.X.; resources, C.F. and M.W.; data curation, Z.X. and J.Z.; writing—original draft preparation, C.S. and Q.R.; writing—review and editing, M.Z., M.A.I.R. and M.W.; visualization, C.S., Y.L. and Z.X.; supervision, M.Z., J.L. and M.W.; project administration, C.F., M.W.; funding acquisition, C.S. and M.W. All authors have read and agreed to the published version of the manuscript.

Funding: This research was funded by the Graduate Student Innovation Ability Training Funding Program of Guangzhou University, grant number 2023GDJC; the Guangdong Basic and Applied Basic Research Foundation, China, grant number 2023A1515030158; and the Guangzhou City School (Institute) Enterprise Joint Funding Project, China, grant number 2024A03J0317.

Data Availability Statement: The study did not report any publicly archived datasets.

Conflicts of Interest: The authors declare no conflicts of interest.

References

1. Yuan, S.H.; Ren, Z.G.; Shan, X.F.; Deng, Q.L.; Zhou, Z. Seasonal different effects of land cover on urban heat island in Wuhan's metropolitan area. *Urban Clim.* **2023**, *49*, 101547. [CrossRef]
2. Zhao, S.H.; Liu, M.; Tao, M.H.; Zhou, W.; Lu, X.Y.; Xiong, Y.J.; Li, F.; Wang, Q. The role of satellite remote sensing in mitigating and adapting to global climate change. *Sci. Total Environ.* **2023**, *904*, 166820. [CrossRef] [PubMed]
3. Yavasli, D.D.; Erlat, E. Climate model projections of aridity patterns in Turkiye: A comprehensive analysis using CMIP6 models and three aridity indices. *Int. J. Climatol.* **2023**, *43*, 6207–6224. [CrossRef]
4. He, H.; Li, R.; Pei, J.; Bilodeau, J.-P.; Huang, G. Current overview of impact analysis and risk assessment of urban pluvial flood on road traffic. *Sustain. Cities Soc.* **2023**, *99*, 104993. [CrossRef]

5. Yuan, H.J.; Wang, M.; Li, J.J.; Zhang, D.Q.; Ikram, R.M.A.; Su, J.; Zhou, S.Q.; Wang, Y.K.; Zhang, Q.F. Matrix scenario-based urban flooding damage prediction via convolutional neural network. *J. Environ. Manag.* **2024**, *349*, 119470. [CrossRef]
6. Kim, J.; Kang, J. Development of hazard capacity factor design model for net-zero: Evaluation of the flood adaptation effects considering green-gray infrastructure interaction. *Sustain. Cities Soc.* **2023**, *96*, 104625. [CrossRef]
7. Yimer, E.A.; De Trift, L.; Lobkowicz, I.; Villani, L.; Nossent, J.; van Griensven, A. The underexposed nature-based solutions: A critical state-of-art review on drought mitigation. *J. Environ. Manag.* **2024**, *352*, 119903. [CrossRef] [PubMed]
8. Acosta-Coll, M.; Ballester-Merelo, F.; Martinez-Peiró, M.; De la Hoz-Franco, E. Real-Time Early Warning System Design for Pluvial Flash Floods-A Review. *Sensors* **2018**, *18*, 2255. [CrossRef]
9. Hu, L.T.; Meng, J.; Xiong, C.Y.; Fang, W.; Yang, J.X.; Liu, M.M.; Bi, J.; Ma, Z.W. City-level resilience to extreme weather shocks revealed by satellite nighttime lights in China. *Sustain. Cities Soc.* **2024**, *101*, 105167. [CrossRef]
10. Wee, G.; Chang, L.C.; Chang, F.J.; Amin, M.Z.M. A flood Impact-Based forecasting system by fuzzy inference techniques. *J. Hydrol.* **2023**, *625*, 130117. [CrossRef]
11. Hu, H.; Tian, Z.; Sun, L.; Wen, J.; Liang, Z.; Dong, G.; Liu, J. Synthesized trade-off analysis of flood control solutions under future deep uncertainty: An application to the central business district of Shanghai. *Water Res.* **2019**, *166*, 115067. [CrossRef] [PubMed]
12. Qiao, X.J. Maintenance of low impact development facilities: A case study of pilot sponge cities in China. *J. Clean. Prod.* **2023**, *425*, 139008. [CrossRef]
13. Tamm, O.; Saaremäe, E.; Rahkema, K.; Jaagus, J.; Tamm, T. The intensification of short-duration rainfall extremes due to climate change-Need for a frequent update of intensity-duration-frequency curves. *Clim. Serv.* **2023**, *30*, 100349. [CrossRef]
14. Li, S.S.; Leitao, J.P.; Wang, Z.L.; Bach, P.M. A drainage network-based impact matrix to support targeted blue-green-grey stormwater management solutions. *Sci. Total Environ.* **2024**, *912*, 168623. [CrossRef] [PubMed]
15. D'Ambrosio, R.; Longobardi, A. Adapting drainage networks to the urban development: An assessment of different integrated approach alternatives for a sustainable flood risk mitigation in Northern Italy. *Sustain. Cities Soc.* **2023**, *98*, 104856. [CrossRef]
16. Williams, J.B.; Jose, R.; Moobela, C.; Hutchinson, D.J.; Wise, R.; Gaterell, M. Residents' perceptions of sustainable drainage systems as highly functional blue green infrastructure. *Landsc. Urban Plan.* **2019**, *190*, 103610. [CrossRef]
17. Xia, J.; Zhang, Y.Y.; Xiong, L.H.; He, S.; Wang, L.F.; Yu, Z.B. Opportunities and challenges of the Sponge City construction related to urban water issues in China. *Sci. China-Earth Sci.* **2017**, *60*, 652–658. [CrossRef]
18. Zhu, S.; Li, D.; Feng, H.; Zhang, N. The influencing factors and mechanisms for urban flood resilience in China: From the perspective of social-economic-natural complex ecosystem. *Ecol. Indic.* **2023**, *147*, 109959. [CrossRef]
19. Zhang, C.; Wang, J.; Liu, J.H.; Lv, Y.P.; Chen, J.; Yang, Z.X.; Zhang, N. Performance assessment for the integrated green-gray-blue infrastructure under extreme rainfall scenarios. *Front. Ecol. Evol.* **2023**, *11*, 1242492. [CrossRef]
20. Xu, C.Q.; Tang, T.; Jia, H.F.; Xu, M.; Xu, T.; Liu, Z.J.; Long, Y.; Zhang, R.R. Benefits of coupled green and grey infrastructure systems: Evidence based on analytic hierarchy process and life cycle costing. *Resour. Conserv. Recycl.* **2019**, *151*, 104478. [CrossRef]
21. Alves, A.; Sanchez, A.; Vojinovic, Z.; Seyoum, S.; Babel, M.; Brdjanovic, D. Evolutionary and Holistic Assessment of Green-Grey Infrastructure for CSO Reduction. *Water* **2016**, *8*, 402. [CrossRef]
22. Ortega-Fernández, A.; Martín-Rojas, R.; García-Morales, V.J. Artificial Intelligence in the Urban Environment: Smart Cities as Models for Developing Innovation and Sustainability. *Sustainability* **2020**, *12*, 7860. [CrossRef]
23. Chen, W.J.; Wang, W.Q.; Huang, G.R.; Wang, Z.L.; Lai, C.G.; Yang, Z.Y. The capacity of grey infrastructure in urban flood management: A comprehensive analysis of grey infrastructure and the green-grey approach. *Int. J. Disaster Risk Reduct.* **2021**, *54*, 102045. [CrossRef]
24. Muttil, N.; Nasrin, T.; Sharma, A.K. Impacts of Extreme Rainfalls on Sewer Overflows and WSUD-Based Mitigation Strategies: A Review. *Water* **2023**, *15*, 429. [CrossRef]
25. Zhang, K.; Chui, T.F.M. A review on implementing infiltration-based green infrastructure in shallow groundwater environments: Challenges, approaches, and progress. *J. Hydrol.* **2019**, *579*, 124089. [CrossRef]
26. Wang, M.; Liu, M.; Zhang, D.Q.; Zhang, Y.; Su, J.; Zhou, S.Q.; Bakhshipour, A.E.; Tan, S.K. Assessing hydrological performance for optimized integrated grey-green infrastructure in response to climate change based on shared socio-economic pathways. *Sustain. Cities Soc.* **2023**, *91*, 104436. [CrossRef]
27. Junqueira, J.R.; Serrao-Neumann, S.; White, I. Using green infrastructure as a social equity approach to reduce flood risks and address climate change impacts: A comparison of performance between cities and towns. *Cities* **2022**, *131*, 104051. [CrossRef]
28. Pecharroman, L.C.; Williams, C.; Nylen, N.G.; Kiparsky, M. How can we govern large-scale green infrastructure for multiple water security benefits? *Blue-Green Syst.* **2021**, *3*, 62–80. [CrossRef]
29. Gashu, K.; Gebre-Egziabher, T. Public assessment of green infrastructure benefits and associated influencing factors in two Ethiopian cities: Bahir Dar and Hawassa. *BMC Ecol.* **2019**, *19*, 16. [CrossRef]
30. Joshi, P.; Leitão, J.P.; Maurer, M.; Bach, P.M. Not all SuDS are created equal: Impact of different approaches on combined sewer overflows. *Water Res.* **2021**, *191*, 116780. [CrossRef]
31. Bakhshipour, A.E.; Bakhshizadeh, M.; Dittmer, U.; Haghighi, A.; Nowak, W. Hanging Gardens Algorithm to Generate Decentralized Layouts for the Optimization of Urban Drainage Systems. *J. Water Resour. Plan. Manag.* **2019**, *145*, 04019034. [CrossRef]
32. Zahediasl, A.; Bakhshipour, A.E.; Dittmer, U.; Haghighi, A. Toward Decentralised Sanitary Sewage Collection Systems: A Multiobjective Approach for Cost-Effective and Resilient Designs. *Water* **2021**, *13*, 1886. [CrossRef]

33. Dierkes, C.; Lucke, T.; Helmreich, B. General Technical Approvals for Decentralised Sustainable Urban Drainage Systems (SUDS)-The Current Situation in Germany. *Sustainability* **2015**, *7*, 3031–3051. [CrossRef]
34. Liu, Z.J.; Han, Z.X.; Shi, X.Y.; Liao, X.Y.; Leng, L.Y.; Jia, H.F. Multi-objective optimization methodology for green-gray coupled runoff control infrastructure adapting spatial heterogeneity of natural endowment and urban development. *Water Res.* **2023**, *233*, 119759. [CrossRef] [PubMed]
35. Liu, Z.J.; Xu, C.Q.; Xu, T.; Jia, H.F.; Zhang, X.; Chen, Z.X.; Yin, D.K. Integrating socioecological indexes in multiobjective intelligent optimization of green-grey coupled infrastructures. *Resour. Conserv. Recycl.* **2021**, *174*, 105801. [CrossRef]
36. Shaamala, A.; Yigitcanlar, T.; Nili, A.; Nyandega, D. Algorithmic green infrastructure optimisation: Review of artificial intelligence driven approaches for tackling climate change. *Sustain. Cities Soc.* **2024**, *101*, 105182. [CrossRef]
37. Yigitcanlar, T.; Mehmood, R.; Corchado, J.M. Green Artificial Intelligence: Towards an Efficient, Sustainable and Equitable Technology for Smart Cities and Futures. *Sustainability* **2021**, *13*, 8952. [CrossRef]
38. Ghodsi, S.H.; Zhu, Z.D.; Matott, L.S.; Rabideau, A.J.; Torres, M.N. Optimal siting of rainwater harvesting systems for reducing combined sewer overflows at city scale. *Water Res.* **2023**, *230*, 119533. [CrossRef] [PubMed]
39. Dong, X.Y.; Yi, W.X.; Yuan, P.; Song, Y.H. Optimization and trade-off framework for coupled green-grey infrastructure considering environmental performance. *J. Environ. Manag.* **2023**, *329*, 117041. [CrossRef]
40. Chen, W.J.; Wang, W.Q.; Mei, C.; Chen, Y.S.; Zhang, P.P.; Cong, P.T. Multi-objective decision-making for green infrastructure planning: Impacts of rainfall characteristics and infrastructure configuration. *J. Hydrol.* **2024**, *628*, 130572. [CrossRef]
41. Tansar, H.; Duan, H.F.; Mark, O. A multi-objective decision-making framework for implementing green-grey infrastructures to enhance urban drainage system resilience. *J. Hydrol.* **2023**, *620*, 129381. [CrossRef]
42. Ballarin, A.S.; Anache, J.A.A.; Wendland, E. Trends and abrupt changes in extreme rainfall events and their influence on design quantiles: A case study in Sao Paulo, Brazil. *Theor. Appl. Climatol.* **2022**, *149*, 1753–1767. [CrossRef]
43. Jiao, Z.C.; Alam, M.A.; Yuan, J.H.; Farnham, C.; Emura, K. Prediction of extreme rainfall events in 21st century—The results based on Bayesian Markov Chain Monte Carlo. *Urban Clim.* **2024**, *53*, 101822. [CrossRef]
44. Ballarin, A.S.; Wendland, E.; Zaerpour, M.; Hatami, S.; Neto, A.A.M.; Papalexiou, S.M. Frequency Rather Than Intensity Drives Projected Changes of Rainfall Events in Brazil. *Earths Future* **2024**, *12*, e2023EF004053. [CrossRef]
45. Ren, Y.; Yu, H.P.; Huang, J.P.; Peng, M.; Zhou, J. The Projected Response of the Water Cycle to Global Warming Over Drylands in East Asia. *Earths Future* **2024**, *12*, e2023EF004008. [CrossRef]
46. Gu, X.H.; Zhang, Q.; Singh, V.P.; Song, C.Q.; Sun, P.; Li, J.F. Potential contributions of climate change and urbanization to precipitation trends across China at national, regional and local scales. *Int. J. Climatol.* **2019**, *39*, 2998–3012. [CrossRef]
47. Ye, C.; Dang, T.D.; Xu, X.F.; Stewart, C.J.; Arias, M.E.; Zhang, Y.; Zhang, Q. Coupled effects of future rainfall and land use on urban stormwater drainage system in Tampa, Florida (USA). *Ecol. Indic.* **2023**, *153*, 110402. [CrossRef]
48. Saurav, K.C.; Shrestha, S.; Ninsawat, S.; Chonwattana, S. Predicting flood events in Kathmandu Metropolitan City under climate change and urbanisation. *J. Environ. Manag.* **2021**, *281*, 111894. [CrossRef]
49. Asamoah, Y.; Ansah-Mensah, K. Temporal Description of Annual Temperature and Rainfall in the Bawku Area of Ghana. *Adv. Meteorol.* **2020**, *2020*, 3402178. [CrossRef]
50. Rao, Y.H.; Zhang, J.J.; Wang, K.; Jepsen, M.R. Understanding land use volatility and agglomeration in northern Southeast Asia. *J. Environ. Manag.* **2021**, *278*, 111536. [CrossRef]
51. Zhang, Y.; Zhong, P.A.; Chen, J.; Bing, J.P.; Xu, D.H.; Wang, M.L. Impacts of Climate Change and Human Activities on the Three Gorges Reservoir Inflow. *Water* **2017**, *9*, 957. [CrossRef]
52. Xu, T.; Li, K.; Engel, B.A.; Jia, H.F.; Leng, L.Y.; Sun, Z.X.; Yu, S.L. Optimal adaptation pathway for sustainable low impact development planning under deep uncertainty of climate change: A greedy strategy. *J. Environ. Manag.* **2019**, *248*, 109280. [CrossRef]
53. de Macedo, M.B.; Mendiondo, E.M.; Razzolini, M.T.P.; Goel, N.K.; Arya, D.S.; Kurian, M.; Nardocci, A.C. Multi-stage resilience analysis of the nexus flood-sanitation-public health in urban environments: A theoretical framework. *Urban Water J.* **2023**, *20*, 1713–1730. [CrossRef]
54. Park, J.; Lu, F.C.; Hedgcock, W.M. Relative Effects of Forward and Backward Planning on Goal Pursuit. *Psychol. Sci.* **2017**, *28*, 1620–1630. [CrossRef]
55. Wiese, J.L. *Backward Planning: Examining Consequences of Planning Direction for Motivation*; Wilfrid Laurier University: Waterloo, ON, Canada, 2011.
56. Wiese, J.; Buehler, R.; Griffin, D. Backward planning: Effects of planning direction on predictions of task completion time. *Judgm. Decis. Mak.* **2016**, *11*, 147–167. [CrossRef]
57. Ott, F.; Markovic, D.; Strobel, A.; Kiebel, S.J. Dynamic integration of forward planning and heuristic preferences during multiple goal pursuit. *PLoS Comput. Biol.* **2020**, *16*, 1007685. [CrossRef]
58. Sun, L.X.; Xia, J.; She, D.X. Integrating Model Predictive Control with Stormwater System Design: A Cost-Effective Method of Urban Flood Risk Mitigation During Heavy Rainfall. *Water Resour. Res.* **2024**, *60*, e2023WR036495. [CrossRef]
59. Zamani, Y.; Monfared, S.A.H.; Moghaddam, M.A.; Hamidianpour, M. A comparison of CMIP6 and CMIP5 projections for precipitation to observational data: The case of Northeastern Iran. *Theor. Appl. Climatol.* **2020**, *142*, 1613–1623. [CrossRef]
60. Kushwaha, P.; Pandey, V.K.; Kumar, P.; Sardana, D. CMIP6 Model Evaluation for Mean and Extreme Precipitation Over India. *Pure Appl. Geophys.* **2024**, *181*, 655–678. [CrossRef]

61. Huang, W.R.; Chang, Y.H.; Deng, L.P.; Liu, P.Y. Simulation and Projection of Summer Convective Afternoon Rainfall Activities over Southeast Asia in CMIP6 Models. *J. Clim.* **2021**, *34*, 5001–5016. [CrossRef]
62. Pu, Y.; Liu, H.B.; Yan, R.J.; Yang, H.; Xia, K.; Li, Y.Y.; Dong, L.; Li, L.J.; Wang, H.; Nie, Y.; et al. CAS FGOALS-g3 Model Datasets for the CMIP6 Scenario Model Intercomparison Project (ScenarioMIP). *Adv. Atmos. Sci.* **2020**, *37*, 1081–1092. [CrossRef]
63. Shenzhen Meteorological Bureau; Shenzhen Municipal Planning and Land Resources Commission. *Shenzhen Rainstorm Intensity Formula and Calculation Chart*; Shenzhen Meteorological Bureau: Shenzhen, China, 2015.
64. Wang, J.; Liu, J.; Mei, C.; Wang, H.; Lu, J. A multi-objective optimization model for synergistic effect analysis of integrated green-gray-blue drainage system in urban inundation control. *J. Hydrol.* **2022**, *609*, 127725. [CrossRef]
65. Houle, J.; Roseen, R.; Ballestero, T.; Puls, T.; Sherrard, J. Comparison of Maintenance Cost, Labor Demands, and System Performance for LID and Conventional Stormwater Management. *J. Environ. Eng.* **2013**, *139*, 932–938. [CrossRef]
66. Dong, Y. Performance assessment and design of ultra-high performance concrete (UHPC) structures incorporating life-cycle cost and environmental impacts. *Constr. Build. Mater.* **2018**, *167*, 414–425. [CrossRef]
67. Wang, M.; Sun, C.H.; Zhang, D.Q. Opportunities and challenges in green stormwater infrastructure (GSI): A comprehensive and bibliometric review of ecosystem services from 2000 to 2021. *Environ. Res.* **2023**, *236*, 116701. [CrossRef] [PubMed]
68. Rasmussen, L.V.; Fold, N.; Olesen, R.S.; Shackleton, S. Socio-economic outcomes of ecological infrastructure investments. *Ecosyst. Serv.* **2020**, *47*, 101242. [CrossRef]
69. Bakhshipour, A.E.; Dittmer, U.; Haghighi, A.; Nowak, W. Hybrid green-blue-gray decentralized urban drainage systems design, a simulation-optimization framework. *J. Environ. Manag.* **2019**, *249*, 109364. [CrossRef]
70. Liu, X.W.; Yang, Y.Y.; Jiang, J. The Behavioral Topsis Based on Prospect Theory and Regret Theory. *Int. J. Inf. Technol. Decis. Mak.* **2023**, *22*, 1591–1615. [CrossRef]
71. Zhu, X.Q.; Li, J.P.; Wu, D.S.; Wang, H.Y.; Liang, C.Z. Balancing accuracy, complexity and interpretability in consumer credit decision making: A C-TOPSIS classification approach. *Knowl. Based Syst.* **2013**, *52*, 258–267. [CrossRef]
72. Zhu, X.; Lee, S.Y.; Wen, X.H.; Ji, Z.M.; Lin, L.; Wei, Z.G.; Zheng, Z.Y.; Xu, D.Y.; Dong, W.J. Extreme climate changes over three major river basins in China as seen in CMIP5 and CMIP6. *Clim. Dyn.* **2021**, *57*, 1187–1205. [CrossRef]
73. Hesarkazzazi, S.; Hajibabaei, M.; Bakhshipour, A.E.; Dittmer, U.; Haghighi, A.; Sitzenfrei, R. Generation of optimal (de)centralized layouts for urban drainage systems: A graph-theory-based combinatorial multi-objective optimization framework. *Sustain. Cities Soc.* **2022**, *81*, 103827. [CrossRef]
74. Tao, T.; Wang, J.; Xin, K.; Li, S. Multi-objective optimal layout of distributed storm-water detention. *Int. J. Environ. Sci. Technol.* **2014**, *11*, 1473–1480. [CrossRef]
75. Scott, C.A.; Shrestha, P.P.; Lutz-Ley, A.N. The re-adaptation challenge: Limits and opportunities of existing infrastructure and institutions in adaptive water governance. *Curr. Opin. Environ. Sustain.* **2020**, *44*, 104–112. [CrossRef]
76. Manocha, N.; Babovic, V. Development and valuation of adaptation pathways for storm water management infrastructure. *Environ. Sci. Policy* **2017**, *77*, 86–97. [CrossRef]
77. Buurman, J.; Babovic, V. Adaptation Pathways and Real Options Analysis: An approach to deep uncertainty in climate change adaptation policies. *Policy Soc.* **2016**, *35*, 137–150. [CrossRef]
78. Zhang, Y.; Wang, M.; Zhang, D.Q.; Lu, Z.M.; Bakhshipour, A.E.; Liu, M.; Jiang, Z.Y.; Li, J.J.; Tan, S.K. Multi-stage planning of LID-GREI urban drainage systems in response to land-use changes. *Sci. Total Environ.* **2023**, *859*, 160214. [CrossRef]
79. Casal-Campos, A.; Sadr, S.M.K.; Fu, G.T.; Butler, D. Reliable, Resilient and Sustainable Urban Drainage Systems: An Analysis of Robustness under Deep Uncertainty. *Environ. Sci. Technol.* **2018**, *52*, 9008–9021. [CrossRef]

Disclaimer/Publisher's Note: The statements, opinions and data contained in all publications are solely those of the individual author(s) and contributor(s) and not of MDPI and/or the editor(s). MDPI and/or the editor(s) disclaim responsibility for any injury to people or property resulting from any ideas, methods, instructions or products referred to in the content.